EpoK, a Cytochrome P450 Involved in Biosynthesis of the Anticancer Agents Epothilones A and B. Substrate-Mediated Rescue of a P450 Enzyme†

Hiroshi Ogura,‡ Clinton R. Nishida,‡ Ute R. Hoch,§ Roshan Perera,|| John H. Dawson,|| and Paul R. Ortiz de Montellano*,‡

Department of Pharmaceutical Chemistry, University of California, 600 16th Street, San Francisco, California 94143-2280, Sunesis Pharmaceuticals, 341 Oyster Point Boulevard, South San Francisco, California 94080, and Department of Chemistry and Biochemistry, University of South Carolina, 631 Sumter Street, Columbia, South Carolina 29208

Received May 19, 2004; Revised Manuscript Received August 3, 2004

ABSTRACT: The epothilones are a new class of highly promising anticancer agents with a mode of action akin to that of paclitaxel but with distinct advantages over that drug. The principal natural compounds are epothilones A and B, which have an epoxide in the macrocyclic lactone ring, and C and D, which have a double bond instead of the epoxide group. The epoxidation of epothilones C and D to A and B, respectively, is mediated by EpoK, a cytochrome P450 enzyme encoded in the epothilone gene cluster. Here we report high-yield expression of EpoK, characterization of the protein, demonstration that the natural substrate can prevent—and even reverse—denaturation of the protein, identification of ligands and surrogate substrates, development of a high-throughput fluorescence activity assay based on the H_2O_2-dependent oxidation of 7-ethoxy-4-trifluoromethylcoumarin, and identification of effective inhibitors of the enzyme. These results will facilitate improvements in the yields of epothilones C and D and the engineering of EpoK to prepare novel epothilone analogues. Furthermore, the finding that the denatured enzyme is rescued by the substrate offers a potential paradigm for control of the P450 catalytic function.

The epothilones, natural products isolated from *Sorangium cellulosum*, have high promise as potential anticancer agents (*1*). Their antitumor activity derives from their ability to stabilize microtubules in a manner very similar to that of paclitaxel (*2*). However, the epothilones have two salient advantages over paclitaxel: they are both more soluble in water, which makes them easier and safer to administer (*3*), and even more importantly are active against paclitaxel-resistant cancer cells (*4*). The primary members of the natural epothilone family are epothilones A and B, both of which have an 11,12-epoxide moiety in the macrocyclic ring framework, and epothilones C and D, the olefin precursors of the epoxide products (Figure 1). Of these natural compounds, epothilones C and D are the most promising as anticancer agents because they have the same tubule-stabilizing properties as the epoxide analogues but are less toxic (*5*, *6*).

The epoxidation of epothilones C and D to A and B, respectively, is mediated by EpoK, a cytochrome P450 enzyme identified in the polyketide synthase (PKS) system of *S. cellulosum* (*7*). EpoK is of practical interest because it controls the ratio of epothilones A/B to C/D in cultures expressing the epothilone gene cluster, generally favoring the epoxide product (*8*). Furthermore, molecular engineering of EpoK may allow the production of alternative oxidized epothilone metabolites with novel biological activities. Preliminary expression of EpoK was used to confirm its role in the conversion of epothilones A/B to C/D, respectively, but in these early experiments the protein was not isolated or otherwise characterized (*7*). As reported here, we have expressed the EpoK gene in *Escherichia coli* and have developed a purification protocol for the protein. We have spectroscopically and kinetically characterized the protein, have developed a high-throughput assay using a surrogate substrate that can be used to screen ligands and inhibitors of the protein, have carried out a brief survey of the enzyme specificity, and have identified inhibitors of the enzyme of potential utility in altering the ratio of the epothilone products in cell culture. In an earlier paper, we reported crystallization and determination of the structures of EpoK in the substrate-free, substrate-bound, and product-bound states (*9*). Our current results reveal an unusual role of the normal substrate in reversibly stabilizing the proximal thiolate ligand that is coordinated to the heme iron atom.

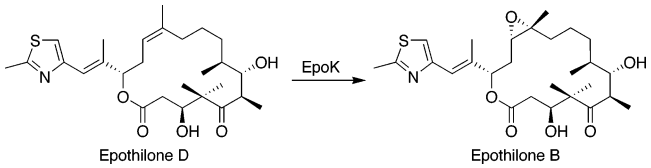

FIGURE 1: EpoK-mediated epoxidation of epothilone D to B.

EXPERIMENTAL PROCEDURES

Materials. The *E. coli* BL21(DE3) strain was purchased from Stratagene (La Jolla, CA). Lysozyme, DNAse, RNAse, and superoxide dismutase (SOD) were from Sigma (St.

† This work was supported by Grant GM25515 (P.R.O.d.M.) from the National Institutes of Health, by BioStar Grant 00-10100 (P.R.O.d.M.) funded by the State of California and Kosan Biosciences, and by Grant GM26730 (J.H.D.) from the National Institutes of Health.

* To whom correspondence should be addressed. Phone: (415) 476-2903. Fax: (415) 502-4728. E-mail: ortiz@cgl.ucsf.edu.

‡ University of California.

§ Sunesis Pharmaceuticals.

|| University of South Carolina.

10.1021/bi048980d CCC: $27.50 © 2004 American Chemical Society
Published on Web 10/28/2004

Louis, MO). The following reagents were used as received: ampicillin, ethylenediaminetetraacetic acid disodium salt (EDTA),[1] and imidazole (Fisher, Pittsburgh, PA), δ-aminolevulinic acid, tris(hydroxymethyl)aminomethane (Tris), β-mercaptoethanol, antipain, leupeptin, pepstatin, phenylmethylsulfonyl fluoride (PMSF), dithiothreitol (DTT), KH_2PO_4, K_2HPO_4, H_2O_2 (30% aqueous solution), miconazole sulfate, econazole sulfate, clotrimazole, sulconazole, and SKF96365 (Sigma), 1-benzylimidazole and 1-(triphenylmethyl)imidazole (Aldrich), isopropyl β-D-thiogalactopyranoside (IPTG; Promega, Madison, WI), glycerol (Acros, Morris Plains, NJ), 7-ethoxy-4-trifluromethylcoumarin (EFC; Molecular Probes, Eugene, OR), ketoconazole (BioMol, Plymouth Meeting, PA), itraconazole (Research Diagnostics, Flanders, NJ), fluconazole (ChemPacific, Baltimore, MD), and fluotrimazole (Riedel-de Haën, Seelze, Germany). The chromatography matrixes Q-Sepharose Fast Flow (FF) (Amersham Biosciences, Piscataway, NJ) and Ni−NTA agarose (Qiagen, Valencia, CA) were loaded and equilibrated with the elution buffer of choice at 4 °C.

Protein Preparation. The expression vector for EpoK was provided by Bryan Julien (Kosan Biosciences, Hayward, CA). This vector is based on pCWori, and encodes a $(His)_6$ tag at the N-terminus of the protein. The gene is flanked by *Nde*I and *Hind*III restriction sites. A 100 μL aliquot of BL21 suspension was transformed with 1 ng of the expression vector according to the instructions from the manufacturer. A 20 μL aliquot of the resulting culture was spread on an LB/ampicillin agar plate and incubated overnight at 37 °C. One of the resulting colonies was used to make an overnight culture in LB containing 100 μg/mL ampicillin. Terrific broth (1 L, containing 100 μg/mL ampicillin) was inoculated with the overnight culture, and the cells were grown at 37 °C (incubator at 225 rpm) until OD = 0.6. At this point, 80 μg/mL δ-aminolevulinic acid was added, and the cells were then induced with 0.5 mM IPTG. The cell suspension was shaken at 25 °C (225 rpm) for 24 h. The suspension was then centrifuged at 6000 rpm for 20 min, and the cell mass (9 g) was recovered and frozen at −70 °C.

The frozen cells were resuspended in a mixture (5 mL/g of cells) of buffer Q (10 mM Tris−Cl, pH 7.5, 10% (v/v) glycerol, 5 mM β-mercaptoethanol, 5 mM imidazole, 1 μg/mL antipain, leupeptin, pepstatin, 20 μg/mL PMSF), lysosyme (0.5 mg/mL), DNAse (50 μg/mL), and RNAse (50 μg/mL). The cells were then lysed using a sonicator, at a temperature no higher than 15 °C. The suspension was then centrifuged at 30000 rpm for 30 min to recover the supernatant.

The supernatant was diluted with 2 volumes of buffer Q, and was then loaded onto a Q-Sepharose FF column (2.5 × 20 cm). The protein was washed with 4 column volumes of buffer Q and then eluted with a NaCl gradient of 200 mL, 0 mM, to 200 mL, 200 mM. The recovered protein was then loaded onto a Ni−NTA column (2.5 × 10 cm), washed with 4 column volumes of buffer N (50 mM Tris−Cl, pH 7.5, 10% (v/v) glycerol, 5 mM imidazole, 5 mM β-mercaptoethanol, 500 mM NaCl, 1 μg/mL antipain, leupeptin, pepstatin, 20 μg/mL PMSF), and then eluted with an imidazole gradient of 100 mL, 5 mM, to 100 mL, 200 mM.

The protein solution was dialyzed twice against 4 L of the storage buffer (50 mM Tris−Cl, pH 7.5, 1 mM DTT, 5 mM imidazole, 1 mM EDTA, 100 mM NaCl), then concentrated to 20 mg/mL EpoK, transferred to 0.5 mL Eppendorf tubes in 100 μL aliquots, frozen, and stored at −70 °C. The amount of protein isolated was 70 mg/L of growth culture.

Formation of the Fe(II)−CO Complex. An anaerobic cuvette was used for this series of experiments. To the buffer (50 mM KP_i, pH 7.4, 100 mM KCl, 0.5 mM EDTA, 600 μL) in the anaerobic cuvette was added 5 μM EpoK. Then, epothilone D (15 μM, from the stock 20 mM solution in DMSO) was added. The cuvette was then placed in the UV/vis spectrophotometer, and the spectrum was taken at 22 °C. The cuvette was then placed on ice and was purged with N_2 for 30 min. Sodium dithionite (100 μM) was added to the solution. The spectrum was then taken at 22 °C. The cuvette was then again placed on ice, and was purged with CO for 30 min. Spectra were taken of the solution at 22 °C in 5 min intervals over the next 2 h. In a separate experiment, the anaerobic cuvette containing the EpoK solution without epothilone D was purged with CO, the solution was treated with dithionite, and spectra were recorded over the next 2 h.

MCD Measurements. The conditions for preparing the ferrous P420− and P450−CO complexes for MCD measurements were the same as used for the absorption spectral studies, except for an increased concentration of EpoK (50−60 μM), glycerol (8% v/v), and epothilone D (40−125 μM). Samples of Mb (∼50 μM) and $P450_{cam}$ were prepared in 100 mM KP_i (pH 7.0) and of CCP (60−83 μM) in 50 mM KP_i (pH 8.0) containing 50 mM KCl. Ferrous samples of all the heme proteins were prepared by addition of 2 μL of 115 mM $Na_2S_2O_4$ solution under N_2. The ferrous−CO and ferrous−NO adducts were generated by addition of $Na_2S_2O_4$, addition of tetrahydrothiophene or cyclopentanethiol in Mb or in the presence or absence of epothilone D in P450 EpoK, and then gentle bubbling of CO and NO under N_2. The MCD data were taken at 4 °C with a JASCO J600A spectropolarimeter in a 0.1 cm cuvette at a magnetic field of 1.41 T. Absorption data were taken of the same samples.

Binding Studies. The binding of substrates to EpoK was observed at room temperature by UV/vis spectrometry, using 400−1000 μL of the measurement buffer (50 mM KP_i, pH 7.4, 100 mM KCl, 0.5 mM EDTA) and 1−5 μM EpoK per cuvette. The spectrometer used was a Cary 1E (Varian, Palo Alto, CA). To obtain a difference spectrum, two cuvettes containing the sample were placed in the spectrometer and the baseline signal was taken. The substrate dissolved in an appropriate organic solvent was added to the sample cuvette, and an equal amount of the solvent was added to the reference cuvette. The spectrum was then recorded from 250 to 800 nm. The titration was continued until there was no further change in the spectrum. The solvent concentration did not exceed 2% (v/v).

The absorbance difference between the maximum and the minimum was calculated for each spectrum. A double-inverse plot of the difference versus the substrate concentration was made, and the *x* intercept was calculated to determine the K_s value (Lineweaver−Burke method).

[1] Abbreviations: Mb, equine myoglobin; $P450_{cam}$, CYP101; CCP, cytochrome *c* peroxidase; MCD, magnetic circular dichroism; EDTA, ethylenediaminetetraacetic acid disodium salt; EFC, 7-ethoxy-4-trifluromethylcoumarin.

Kinetic Studies of Epothilone D Epoxidation by EpoK. The reactions were performed at room temperature. Epothilone D solution in DMSO (10 mM) was serially diluted seven times, each step consisting of 2-fold dilution. A 4 μL aliquot of each epothilone D solution was added to 800 μL of 100 mM KP_i, pH 7.4, buffer containing 0.2 μM EpoK, 20 μg/mL ferredoxin, 0.0025 U/mL ferredoxin reductase, 1.3 mM NADPH, and NADPH regeneration system (0.4 U/mM G6P dehydrogenase, 3.3 mM glucose-6-phosphate). From each reaction mixture, a 100 μL aliquot was removed at 0, 3, 6, 9, 12, 15, and 20 min from the start of the reaction, and was quenched with MeCN/6% (v/v) HOAc. The precipitate was removed, and the supernatant was used for analysis.

The HPLC analysis was performed using a Hewlett-Packard HP1090 chromatograph and a Metachem C18 Polaris column (2.1 × 50 mm, 5 μm). The solvents used were 0.05% (v/v) HOAc in water (solvent A) and 0.05% HOAc in acetonitrile (solvent B). The oven temperature was set at 40 °C, and the flow rate at 0.3 mL/min. The gradient was set as follows: keep at 30% B from 0 to 0.5 min, raise to 50% B by 1 min, keep there until 2.5 min, raise to 90% B by 5 min, lower to 30% B by 6 min, and keep there until 10 min. The areas under the product and the substrate peaks were used to calculate the molar concentration of the product at each time point. The product concentration vs time plot was made, the rates were calculated, and the Michaelis−Menten constants were determined.

Similar reaction and analysis conditions were used for the inhibition experiment with econazole. The enzyme concentration was 0.5 μM, the epothilone D concentration was fixed at 1 μM, the econazole concentrations were varied from 0.016 to 10 μM, and the total DMSO concentration was kept at 0.2% (v/v).

Fluorescence Detection and Analysis of Kinetic Data. The reaction was performed in a 96-well plate (280 μL capacity, U-shaped bottom). All the reactions were performed in duplicate, except for those containing no inhibitors and those containing no H_2O_2, which were performed in sextuplicate. The inhibitor was serially diluted in a row of 12 wells so that the concentration would cover at least 2 decades. Multichannel pipettors were used for filling the wells with reaction mixtures, appropriately diluted inhibitors, and H_2O_2. These pipettors allowed for fewer errors in reagent manipulation and a faster assay.

The reaction buffer contained 50 mM KP_i, pH 7.4, 100 mM KCl, 0.5 mM EDTA, 10 U/μL SOD, and 3−5 μM EpoK. EFC (20 mM stock solution in acetonitrile) was added so that the concentration was 100 μM EFC, 0.5% (v/v) acetonitrile. The reaction mixture (150 μL) was placed in the plate wells using a 12-channel pipettor. The inhibitor at an appropriate concentration in acetonitrile (0.75 μL) was then added to the reaction mixtures. The final acetonitrile concentration was 1% (v/v). The reaction was started by adding 3 μL of 50 mM H_2O_2, which made the final H_2O_2 concentration 1 mM.

The reaction was monitored using a SpectraMax Gemini XS (Molecular Devices, Sunnyvale, CA) 96-well plate fluorometric reader. The wavelengths were set at 409 nm excitation/530 nm emission/475 nm cutoff. The bandwidth had been set by the factory to 9 nm. The reaction was monitored for 60 min, with fluorescence measured every 30−40 s. The plate was shaken for at least 8 s between measurements. The temperature was kept at 25 °C.

The resulting fluorescence was plotted against time, and the slope was determined. The rate was plotted against the inhibitor concentration, and fitted to the following tight-binding equation to determine $K_{i,apparent}$ (*10*):

$$v = v_0 \frac{([I] + K_{i,apparent} - [EpoK]) - [([I] + K_{i,apparent} - [EpoK])^2 + 4[EpoK]K_{i,apparent}]^{1/2}}{2[EpoK]}$$

This equation, at the limit of [EpoK] = 0, becomes the conventional dose−response equation, with $K_{i,apparent}$ becoming IC_{50}.

RESULTS

Protein Preparation. In contrast to previous work in which expression of EpoK resulted in the formation of inclusion bodies and a low yield of the functional protein (*7*), expression of EpoK in *E. coli* using the pCWori-based expression vector yielded soluble protein in an excellent yield of approximately 70 mg/L. As found for most P450 enzymes, the pCWori vector is well suited for the expression of EpoK. The protein, purified by sequential Q-Sepharose and Ni−NTA chromatography, was shown by SDS−PAGE gel electrophoresis to be pure (Figure 2, upper inset). The high degree of purity is confirmed by the fact that the protein obtained by this procedure has been crystallized and the crystal structure has been successfully determined (*9*).

Spectroscopic Properties. Ferric EpoK has an absorption maximum at 418 nm in the hexacoordinated, water-bound state. When dithionite is added to EpoK, the absorption maximum shifts to 414 nm with some broadening of the band and a slight decrease in intensity (Figure 2, top). When CO is added to dithionite-reduced EpoK, the resulting spectrum shows significant quantities of two species, one absorbing at 422 nm and the other at 448 nm. The initial ratio of the intensities of these two peaks varies from experiment to experiment, but it is generally found that the 422 nm peak increases with time. This indicates that the ferrous protein in the absence of an epothilone substrate undergoes a time-dependent denaturation that results in loss of the characteristic absorption maximum of the Fe(II)−CO complex at ∼450 nm in favor of a species with a Soret maximum at 422 nm.

Epothilone D, one of the natural substrates, stabilizes the protein against this denaturation. This is demonstrated by an experiment in which EpoK, epothilone D, a N_2 purge, sodium dithionite, and finally a CO purge are added, in that order, to the assay buffer in an anaerobic cuvette. Addition of the epothilone D caused the Soret band to shift to 414 nm (Figure 2, bottom). Upon further addition of dithionite, the Soret band did not change in wavelength or bandwidth but its intensity decreased. Introduction of CO then caused the appearance of a peak at 446 nm that gradually increased at the expense of the peak at 414 nm. The reaction with CO was slow and was not complete after 2 h, but the spectrum taken after 15 h exhibited primarily the 446 nm peak with only a smaller peak at 422 nm.

More surprising than stabilization of the P450 structure by a ligand is the finding that addition of epothilone D, the

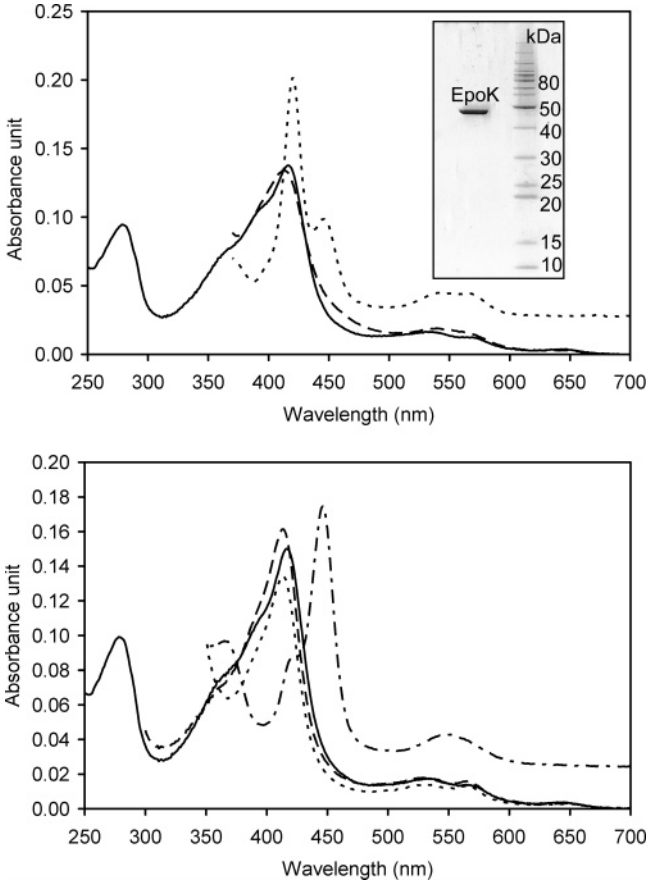

FIGURE 2: Spectra of EpoK (room temperature, 50 mM KP_i, pH 7.4, 100 mM KCl, 0.5 mM EDTA). Upper panel: (a) Fe(III) EpoK (—) with a Soret maximum at 418 nm; (b) Fe(II) EpoK obtained by reaction with sodium dithionite (− − −) with a maximum at 414 nm; (c) Fe(II)−CO EpoK complex (---) with a major peak at 422 nm and a minor peak at 448 nm. The inset shows the SDS−PAGE electrophoresis gel (10% acrylamide, denaturing conditions, Coomassie Blue staining) of EpoK alongside a molecular weight ladder. Lower panel: (a) Fe(III) EpoK (—) with the Soret peak at 418 nm; (b) Fe(III) EpoK−epothilone D complex (---) with a maximum at 414 nm; (c) EpoK−epothilone D complex after treatment with sodium dithionite (− − −), peak at 414 nm; (d) Fe(II)−CO EpoK complex (-·-·-) with a major peak at 446 nm and a minor peak at 423 nm.

native substrate, to the preformed P420−CO complex reverses the denaturation process (Figure 3). This unprecedented substrate-mediated rescue of the denatured protein only occurs if the reaction is carried out at low temperature (∼15 °C) or the solution contains at least 1% (v/v) glycerol. A final P420:P450 peak height ratio of approximately 1:3 is obtained, the same ratio that is observed when epoK is reduced in the presence of both CO and epothilone D.

Epothilone D causes an unusual change in the EpoK spectrum in that its binding increases rather than decreases the absorbance at 410 nm (Figure 4). Thus, instead of causing a shift from the low-spin hexacoordinated state to the high-spin pentacoordinated state, as is observed on substrate binding to most P450 enzymes, binding of the native substrate to EpoK appears to increase the concentration of the low-spin hexacoordinated protein. This suggests that the substrate, instead of sterically displacing the distal water ligand, either stabilizes it or substitutes for it.

Magnetic Circular Dichroism. To determine the coordination structure of the ferrous−CO and −NO protein in the

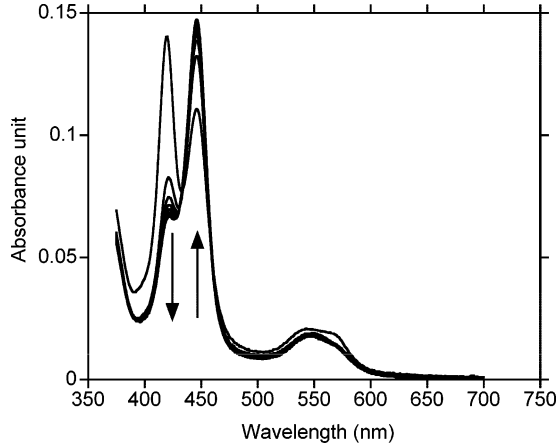

FIGURE 3: Conversion of the P420 species (1 μM) into a P450 species upon addition of 20 μM epothilone D to the substrate-free Fe(II)−CO complex at room temperature (1% (v/v) glycerol, 50 mM KP_i, pH 7.4, 100 mM KCl, 0.5 mM EDTA), with spectra taken at 10 min intervals.

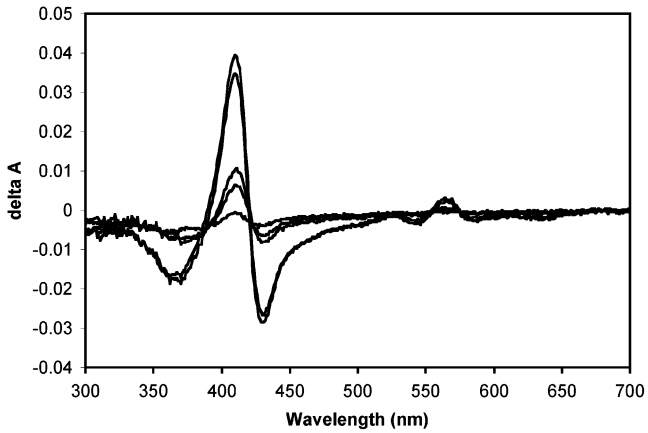

FIGURE 4: Difference spectra for epothilone D binding to Fe(III) EpoK at room temperature. The buffer composition is the same as the one for Figure 2. The increasing epothilone D concentrations were 0.2, 0.6, 0.8, 3, and 7 μM. Note the increase in the H_2O-bound low-spin heme signal at 410 nm.

presence and absence of the substrate, we have employed MCD spectroscopy (Figures 5−8). The information provided by MCD measurements of ferroheme proteins generally depends on the identity of the axial ligands. When the distal ligand is CO, the MCD spectra exhibit relatively small differences with changes in the proximal ligand other than for thiolate (cysteinate) ligation. When the distal ligand is NO, the MCD spectra easily differentiate between five- and six-coordinate species. With six-coordinate ferrous−NO complexes, the MCD spectra can distinguish between nitrogen and sulfur proximal ligands, and with sulfur proximal ligands, the technique can differentiate between neutral (thiol) and anionic (thiolate) ligands (*11*−*13*).

As shown in Figures 5 and 6, one can estimate the ratio of the thiol- to the thiolate-coordinated forms by simulating both the observed MCD and absorption data from the known spectra of pure P420 and P450 species.The P420 species was simulated by using the data from H715C/D235L cytochrome *c* peroxidase (CCP), H93G myoglobin (Mb)−cyclopentanethiol complex, and H93G Mb−tetrahydrothiophene complex. All of these species, upon reduction and coordination with CO, produce ferrous 6-coordinated species with a thiol or thioether ligand (*12*). The P450 species was simulated

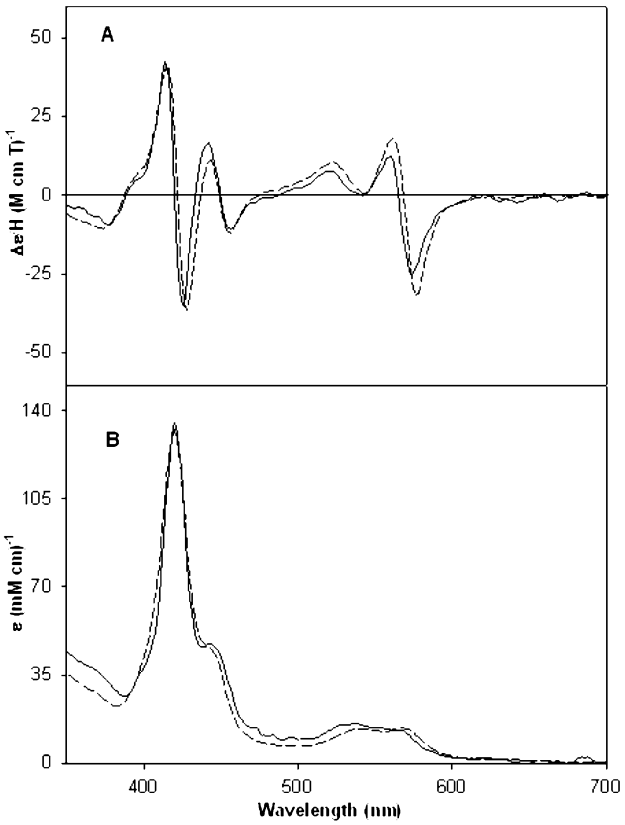

FIGURE 5: MCD (A) and electronic absorption (B) spectra of Fe(II)−CO EpoK (substrate free) (solid line) and simulated MCD spectrum of Fe(II)−CO H175C/D235L CCP (76%) plus Fe(II)−CO $P450_{cam}$ (24%) (dashed line). All the MCD spectra were taken at 4 °C; see the Experimental Procedures for the complete conditions. The $P450_{cam}$ and cytochrome *c* peroxidase data were taken from refs *12* and *11*, respectively.

with the data from $CYP450_{cam}$. The MCD and absorption spectra from the same data set were simulated using the same P420:450 ratio. The simulations indicated that, for the substrate-free form, the ratio was 76% thiol and 24% thiolate and, for the substrate-bound form, the ratio was 20% thiol and 80% thiolate.

Although the MCD of ferrous CO-coordinated samples does not independently define the state of the proximal ligand in the P420 species derived from EpoK, it is still useful when, as here, one has a fair degree of confidence that the proximal ligand is a sulfur atom. Retention of the thiol is more consistent with the reversible nature of the P450−P420 interconversion than complete exchange of the ligand. The interconversion therefore probably involves protonation of the P450 thiolate ligand to give a thiol ligand.

Binding of NO to ferric EpoK yields complexes with absorption maxima at 431 nm. Addition of NO to ferrous P450 EpoK generates complexes that further support the idea of interconvertible neutral (thiol) and anionic (thiolate) proximal coordination. The MCD and UV/vis absorption spectra of ferrous−NO P450 EpoK in the absence of epothilone D show that it is a five-coordinate complex with spectral features very similar to those of the five-coordinated H93G Mb−NO adduct (Figure 7). On the other hand, addition of substrate plus NO to ferrous P450 EpoK or addition of substrate to ferric−NO P450 EpoK followed by reduction gives a six-coordinated species with an MCD spectrum comparable to that of the ferrous−NO H93G-

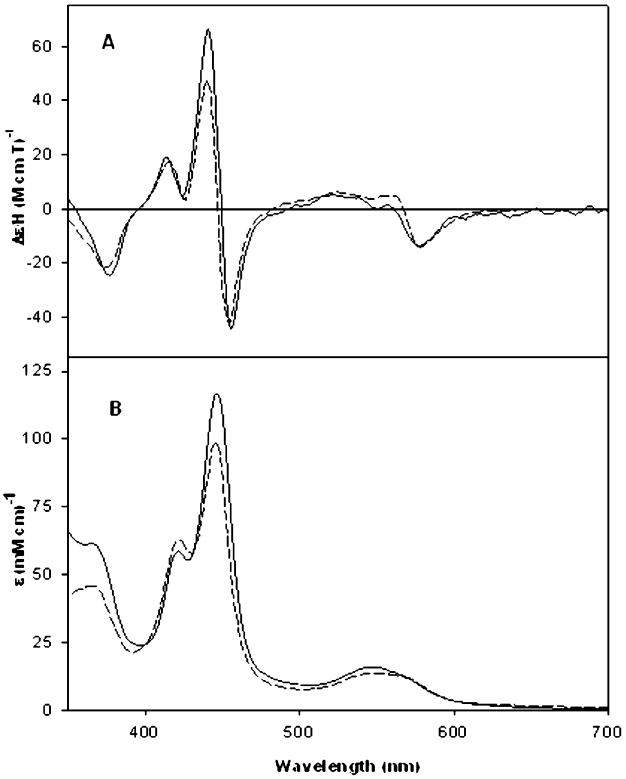

FIGURE 6: MCD (A) and electronic absorption (B) spectra of Fe(II)−CO EpoK in the presence of epothilone D as substrate (solid line) and simulated MCD spectrum of Fe(II)−CO H175C/D235L CCP (20%) plus Fe(II)−CO $P450_{cam}$ (80%) (dashed line). The $P450_{cam}$ and cytochrome *c* peroxidase data were taken from refs *13* and *12*, respectively.

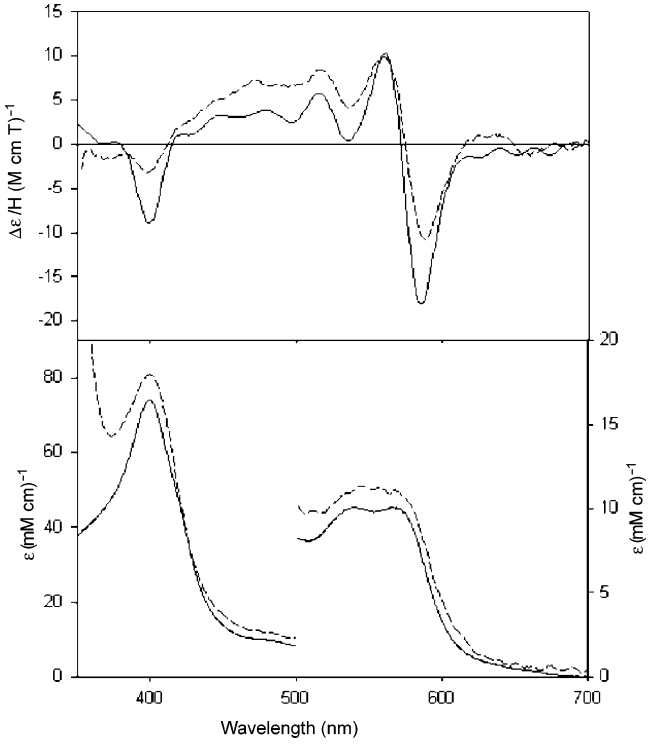

FIGURE 7: MCD (A, top) and electronic absorption (B, bottom) spectra of Fe(II)−NO P450 EpoK (substrate free) (solid line) and ferrous−NO H93G Mb (dashed line). The H93G spectrum is replotted from data in ref *11*.

(tetrahydrothiophene) Mb complex (Figure 8). As the latter complex contains a neutral sulfur donor ligand, we conclude

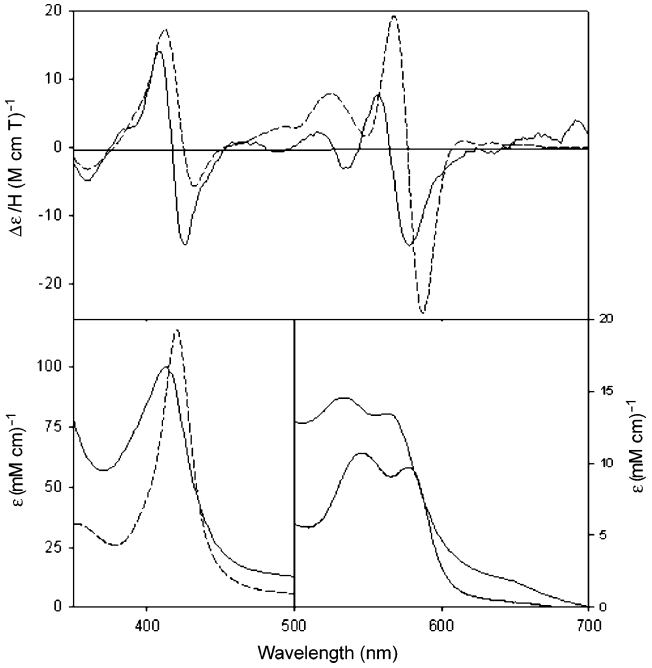

FIGURE 8: MCD (A, top) and electronic absorption (B, bottom) spectra of Fe(II)−NO P450 EpoK in the presence of epothilone D (solid line) and ferrous−NO H93G(Im) (dashed line). The H93G spectrum is replotted from data in ref *11*.

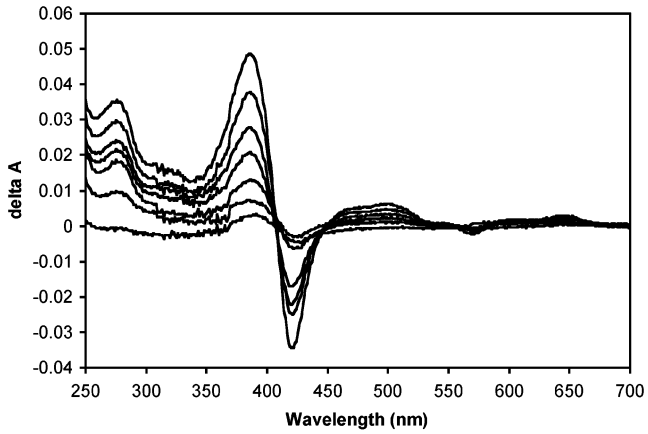

FIGURE 9: Difference spectra for *n*-decanoic acid (C_{10}) binding. All the binding experiments were performed at room temperature, with buffer whose composition was the same as the one used for Figure 2. The EpoK concentration in this experiment was 3 μM. The C_{10} concentrations were 1.7, 6.6, 74, 250, 420, 580, and 900 μM. The spectral change is of type I, unlike the one for the binding of epothilone D.

that ferrous−NO P450 EpoK in the presence of substrate is thiol (neutral cysteine)-ligated (Scheme 1).

Ligand Binding Studies. In contrast to kinetic studies described below, in which DMSO was found to inhibit catalytic turnover more extensively than acetonitrile, a ligand dissolved in DMSO was found to bind to EpoK just as well as the same ligand dissolved in acetonitrile. The ligands examined here were the linear fatty acids of different lengths because they are often accepted as ligands by bacterial P450 enzymes and can be used as a first measure of the effective size of the active site cavity (i.e., ref *14*). In fact, the medium-length fatty acids bind to EpoK to give a typical "type I" binding spectrum (Figure 9). This spectrum indicates that the low-spin signal due to the hexacoordinated resting state of the enzyme decreases and the high-spin signal due to the pentacoordinated species increases as the fatty acid concentration is raised. However, these medium-length fatty acids (C_{11}−C_{15}) exhibit biphasic binding behavior (Figure 10, Table 1), in contrast to monophasic binding of the longer chain fatty acids (C_{16}−C_{18}), and the failure of acids greater than C_{20} in length to bind at all. Short-length acids (C_8−C_9) did not cause a spectral change when added to EpoK,

Scheme 1: EpoK Heme Complexes Proposed for the Observed Intermediates and Their Interrelationship

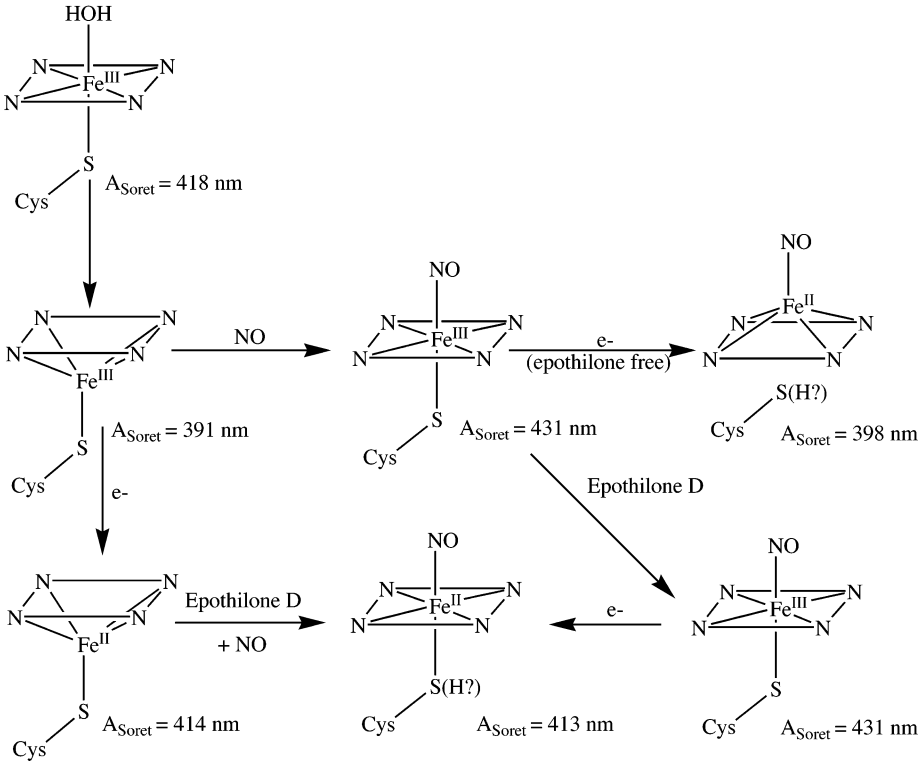

Table 1: Constants for Binding of Linear-Chain Organic Acids to EpoK

acid	binding constant (μM)	"second" binding constant (μM)	acid	binding constant (μM)	"second" binding constant (μM)
C_8	N/A	600 ± 100	C_{16}	2.7 ± 0.1	N/A
C_{10}	5 ± 3	800 ± 100	C_{17}	21 ± 0.6	N/A
C_{12}	1.6 ± 0.4	35 ± 2	C_{18}	too large to calculate by the Lineweaver−Burke method	
C_{14}	3.8 ± 0.1	20 ± 4	C_{20}	not found	
C_{15}	6.4 ± 0.8	39 ± 4			

presumably because they are too small to displace the distal water ligand when bound in the active site.

When EpoK is reduced in the presence of CO and lauric acid instead of epothilone D, only the P420 species is observed. Thus, the stabilization of the ferrous−CO complex by epothilone D is relatively specific for this natural substrate and is not mimicked by the fatty acids.

Reducing Partners and Epoxidation Kinetics. The native electron donor partners of EpoK are not known. We therefore searched for heterologous partners that could be used to investigate the catalytic properties of the enzyme. Putidaredoxin (Pd) and putidaredoxin reductase (PdR) from *Pseudomonas putida*, the partners of $P450_{cam}$, did not support the catalytic turnover of EpoK even when the EpoK:Pd:PdR ratio was varied from 1:2:2 to 1:10:2. In contrast, the epoxidation of epothilone D was catalyzed by EpoK in the presence of spinach ferredoxin, ferredoxin reductase, and NADPH. Using an NADPH-regenerating system consisting of glucose-6-phosphate and glucose-6-phosphate dehydrogenase (G6PDH) to keep the NADPH concentration constant, this system supported the epoxidation of epothilone D with $V_{max} = 0.56$ μM min^{-1} M^{-1} (EpoK) and $K_m = 1.6$ μM.

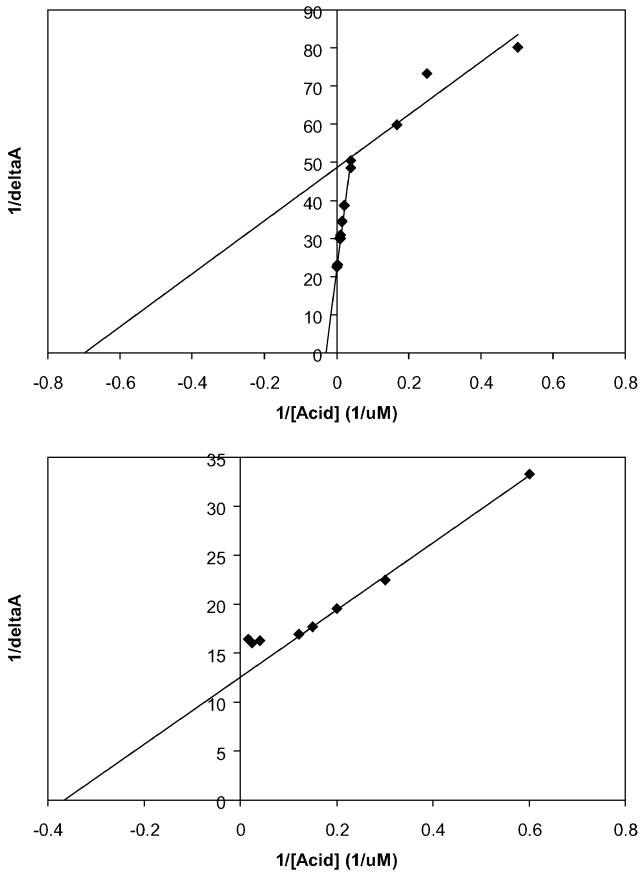

FIGURE 10: Lineweaver−Burke plots for lauric acid (C_{12}, top) and palmitic acid (C_{16}, bottom). The EpoK concentration was 3 μM in both experiments. The C_{12} binding curve shows a biphasic pattern, while that for C_{16} shows a monophasic pattern.

High-Throughput Assay. One goal of this study was to identify inhibitors of EpoK that could be used to improve the yield of epothilone D in fermentation cultures by inhibiting its epoxidation. As the epoxidation of epothilone D is not a convenient assay for the screening of inhibitors, we have developed a high-throughput kinetic assay based on the oxidation of a fluorogenic substrate (*15*−*20*). Initial efforts to develop such an assay using the surrogate electron donors spinach ferredoxin/ferredoxin reductase and putidaredoxin/putidaredoxin reductase were unsuccessful, as even EFC (Figure 11), the substrate eventually employed, was not detectably dealkylated with these electron donor partners. However, EpoK catalytically oxidized this substrate if the electron donor complications were circumvented by employing H_2O_2 as the oxidizing agent. Khan and Halpert recently reported a similar peroxide-based fluorogenic assay for the $P450_{eryF}$ A245T mutant (*21*). The use of the so-called "peroxide shunt" reaction requires a careful titration of the H_2O_2 concentration used in the experiments, as high concentrations of the peroxide degrade the protein and its heme group. A H_2O_2 concentration of 1 mM was found to minimize the damage to the protein.

Although the solvent used to deliver potential ligands did not appear to be critical in the spectroscopic K_s studies (see

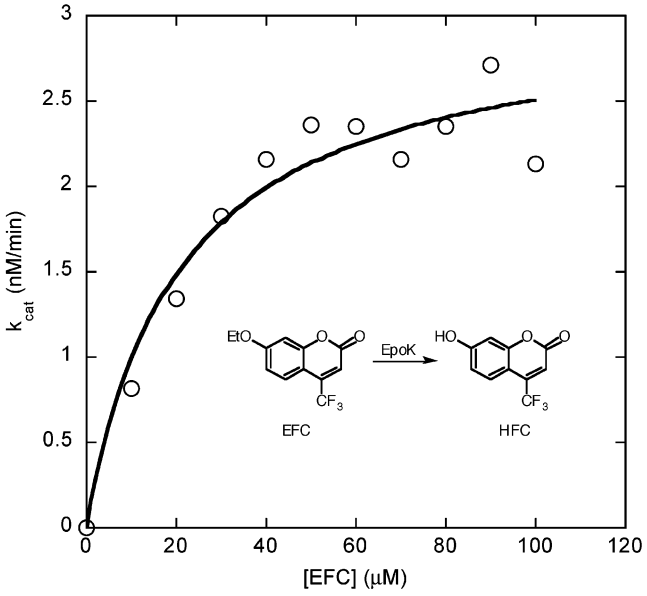

FIGURE 11: Michaelis−Menten plot of EFC dealkylation catalyzed by EpoK (25 °C) (50 mM KP_i, pH 7.4, 100 mM KCl, 0.5 mM EDTA, 10 U/μL SOD, 5 μM EpoK, 1% (v/v) acetonitrile). The EFC reaction yields a fluorescent species (excitation/emission 409/530 nm) which is well suited for a rapid kinetic assay.

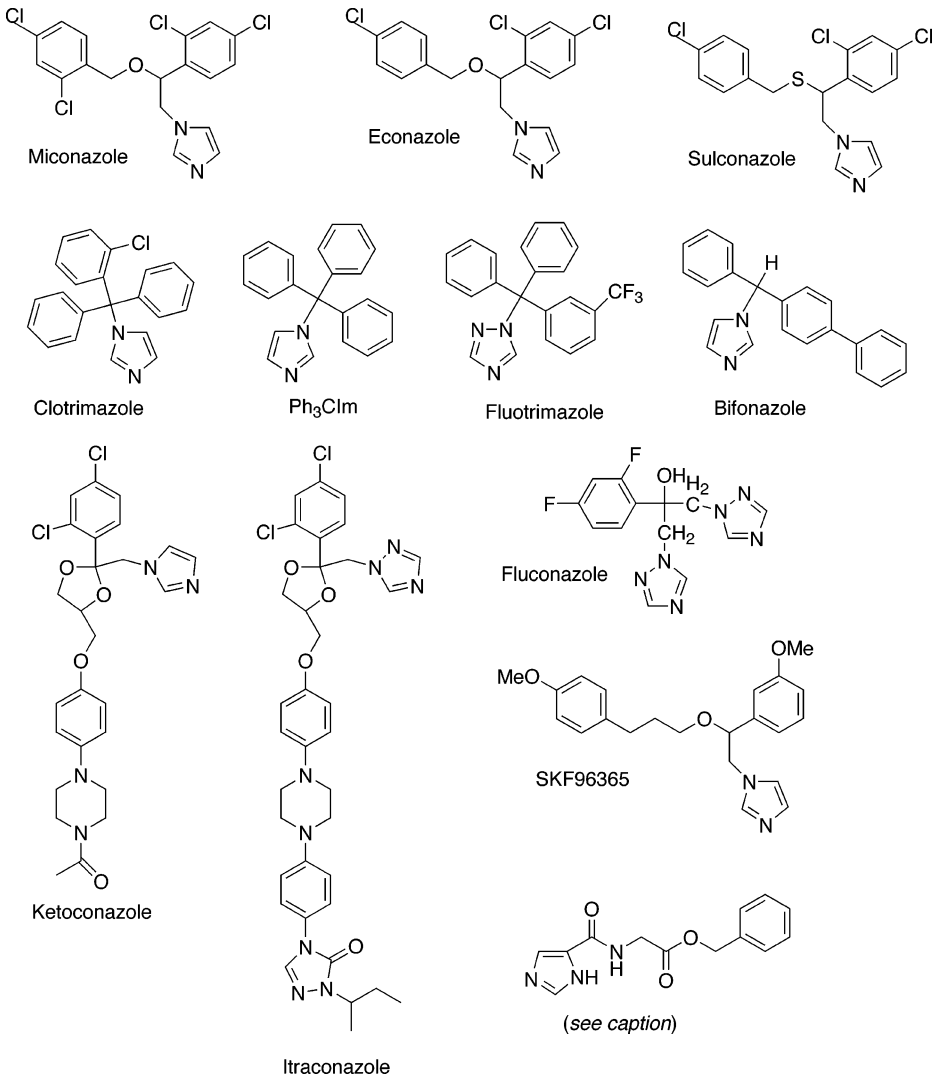

FIGURE 12: Structures of the imidazole-based inhibitors, including one 4-amidoimidazole, examined in this study.

Table 2: $K_{i,apparent}$ Values of EpoK Inhibitors

inhibitor	$K_{i,apparent}$(μM)	inhibitor	$K_{i,apparent}$(μM)
4-phenylimidazole	47 ± 5	econazole	0.5 ± 0.1
clotrimazole	0.2 ± 0.1	SKF96365	1.2 ± 0.3
itraconazole	>10 (solubility in CH_3CN too low)	Ph_3CIm	0.10 ± 0.06
ketoconazole	1.7 ± 0.4	bifonazole	0.16 ± 0.04
fluconazole	>50 (no inhibition observed)	fluotrimazole	0.25 ± 0.06
miconazole	1.8 ± 0.7	1-benzylimidazole	>50 (no inhibition observed)
phenmedipham	34 ± 5	sulfaphenazole	110 ± 20
sulconazole	0.10 ± 0.03	ω-pentadecalactone	12 ± 2

above), it was important for the turnover experiments. When DMSO was used as the solvent, the dealkylation of EFC could not be detected using a fluorometric plate reader, although it could be detected using a cuvette-based fluorimeter. On the other hand, when acetonitrile was used as the solvent, the reaction was readily detected by both methods. The potential inhibitors were therefore delivered in acetonitrile.

Kinetic analysis of the oxidation of EFC using the shunt system gives a Michaelis−Menten plot (Figure 11) from which the values $K_M = 18$ μM and $V_{max} = 0.6$ nM min^{-1} M^{-1} (EpoK) can be calculated.

Inhibitor Identification. Imidazoles and related nitrogen heterocycles which coordinate to the iron atom of P450 enzymes provide the framework for the largest class of P450 inhibitors (*22*). Our efforts to examine imidazole inhibitors were complicated by the necessity of avoiding DMSO because most imidazole-based inhibitors are significantly more soluble in DMSO than in acetonitrile. The upper limit to the inhibitor concentration that could be evaluated was therefore considerably lower when acetonitrile was used instead of DMSO as the solvent. This problem was especially acute with the 4-amidoimidazoles because their low solubility in acetonitrile yielded final inhibitor concentrations that were considerably below the $K_{i,apparent}$. Methanol was therefore used as the solvent in these cases because, although it inhibits the reaction, it does so less than DMSO.

The binding of imidazoles, as expected, gives rise to "type II" difference spectra in which the signal for the amine-coordinated low-spin iron(III) heme complex increases at the expense of the water-coordinated species. An exception was the 2-amidoimidazole, which gave a type I difference spectrum (*23*). The binding of the imidazoles was monophasic, in contrast to that of the fatty acids. The $K_{i,apparent}$ values for a series of imidazoles (Table 2) show that sulconazole is the most effective inhibitor, although related species such as clotrimazole, fluotrimazole, bifonazole, and triphenyl-

methylimidazole have comparable $K_{i,apparent}$ values (Figure 12). The one nonimidazole compound tested, pentadecalactone, is notable because its $K_{i,apparent}$ value is in the low micromolar range even though it cannot coordinate to the heme iron atom (Table 2).

One of the imidazoles, econazole, was tested for inhibition of the epothilone D epoxidation. This inhibitor, whose $K_{i,apparent}$ value for the EFC dealkylation was 0.5 μM, showed a $K_{i,apparent}$ value for the epoxidation of 0.13 μM, and also a K_s value for econazole binding of 0.24 μM. These three values are comparable.

DISCUSSION

The expression and purification of EpoK reported here unambiguously confirm the earlier conclusion that it oxidizes epothilone D to epothilone B in *S. cellulosum* (*7*). This is the first report of the solution properties of EpoK, although crystallization of the protein and determination of its crystal structure were reported in an earlier paper (*9*).

The most remarkable property of EpoK emerging from the present studies is the unusual role of epothilone D, the natural substrate, in stabilizing the ferrous form of the protein. Reduction of the protein to the ferrous state in the absence of this substrate, or in the presence of an unnatural ligand such as lauric acid, results in virtually complete conversion of the thiolate-ligated form, with an Fe(II)−CO absorption maximum at ~450 nm, to a denatured form with the Fe(II)−CO absorption maximum at 422 nm. This "P420" species arises either by simple protonation of the cysteine thiolate, converting it to a thiol ligand, or by actual dissociation of the thiolate ligand from the iron, followed by coordination of an alternative ligand. Formation of the P420 species is normally an irreversible process, although reversion of a pressure-induced P420 species to the P450 form has been reported (*24*, *25*). The finding that epothilone D, but not lauric acid, protects the enzyme from conversion to the P420 form upon reduction requires that the normal ligand suppress reduction-linked structural alterations that occur in its absence. Ligands have been observed previously to stabilize ferric P450 proteins: for example, ligands stabilize CYP2E1 and thus elevate its concentration (*26*), and ligands stabilize heterologously expressed CYP4B1 with respect to its conversion to the P420 form (*27*). However, to our knowledge, no other example is known of the reversion of a preformed P420 Fe(II)−CO complex to the P450 Fe(II)−CO form upon binding of the substrate.

The MCD data suggest that the P420−P450 interconversion involves substrate-dependent protonation−deprotonation of the proximal cysteine thiolate ligand. The crystal structure shows the sulfur−iron bond is of normal length in the ferric protein, thus confirming the thiolate ligation (*9*). This is important, as the only other evidence for thiolate ligation, apart from conservation of this ligand in all known P450 enzymes, is the formation of a ferrous−CO complex absorbing at 450 nm. In view of the crystal structure and of our current data we can exclude the possibility that thiolate ligation is not present in the ferric protein and is only obtained upon reduction of the iron in the presence of epothilone D. Binding of the normal substrate thus functions as a switch that preserves, or reestablishes, the thiolate ligation and enables catalytic turnover. Inspection of the crystal structure of EpoK does not provide an obvious explanation for this unusual behavior.

Two important pieces of information emerge from our analysis of the binding of fatty acids to EpoK. The observation that medium-chain but not long-chain fatty acids bind to the enzyme, as judged by the spectroscopically detectable low-to-high spin shift of the iron atom, provides a sense of the effective dimensions of the active site. Furthermore, the finding that the medium-length fatty acids bind in a biphasic manner indicates either that two binding sites exist for the fatty acids or that a single binding site can accommodate two fatty acid molecules, the first being bound with an affinity different from that of the second. The binding of two substrates within a single active site is not uncommon, as this has been directly demonstrated for P450eryF (*28*, *29*) and is widely inferred from kinetic and other considerations for enzymes such as CYP3A4 (*30*) and CYP2C9 (*31*). Indeed, the EpoK crystal structure shows that the active site cavity is large enough to possibly accommodate two fatty acid molecules (*9*).

Interestingly, although the fatty acids bind to EpoK, they are not detectably oxidized when catalytic turnover of the enzyme is supported by the spinach ferredoxin/ferredoxin reductase surrogate electron donors. However, this finding is readily explained by the finding that the ferrous protein is unstable in the absence of epothilone D and that this instability is not alleviated by either the fatty acids. As the thiolate ligand helps to tune the redox potential of EpoK, it is not surprising that electron transfer to the iron is disrupted when the thiolate ligand is either protonated or displaced. In contrast, the peroxide shunt pathway, which does not require electron transfer to the iron, is relatively insensitive to the nature of the proximal ligand, as peroxide activation can be achieved equally well with histidine-ligated hemoproteins (*32*, *33*). We have made use of this difference to circumvent the defect in electron transfer and have developed a high-throughput catalytic assay that can be used to screen for inhibitors.

The search for inhibitors of EpoK has identified several imidazole derivatives that can be used to improve the yield of epothilone D at the expense of epothilone B in cell culture. The inhibitory potency of the imidazoles correlates to some extent with the lipophilicity of the compounds and the size of their substituents (Table 2). Thus, 1-benzylimidazole, with a small substituent, did not detectably inhibit EpoK, nor did itraconazole, which despite its lipophilicity has a very large substituent. The best inhibitors were found to be those with a triphenylmethyl substituent, such as clotrimazole and 1-triphenylmethylimidazole, or the $-CH_2CH(Ph^1)(ECH_2Ph^2)$ (E = O, S) substituent of sulconazole and econazole.

The nitrogen basicities of all the imidazole inhibitors in Table 1 are approximately the same except for 4-amidoimidazole, in which the pK_a of the nitrogen is greatly decreased by the electron-withdrawing effect of the amide group. This compound did not inhibit EFC dealkylation by EpoK, and the spectroscopic studies showed that the nitrogen did not coordinate to the iron to give a typical type II difference spectrum, but rather gave a type I spectrum.

In summary, EpoK, a new and important enzyme in the biosynthetic pathway to the epothilone anticancer agents, has been expressed, purified, and characterized in terms of its basic spectroscopic and kinetic properties. Fatty acids have

been used to probe the substrate binding site, and a high-throughput assay using H_2O_2 as a surrogate oxidant has been used to identify effective inhibitors of the enzyme. The most unusual property of the enzyme found in this study is the ability of the native substrates to rescue the enzyme from the partially denatured P420 state. Although substrate stabilization of the P450 form relative to conversion to the P420 form has been observed previously, this appears to be the first instance in which addition of the substrate to the P420 form results in reconstitution of the native, catalytically active, P450 state. This link between the native substrate and the protein state may help to limit the participation of the enzyme in the oxidation of extraneous substrates and the production of uncoupled oxidation products.

ACKNOWLEDGMENT

We thank Bryan Julien of Kosan Biosciences, Hayward, CA, for the EpoK plasmid. We also thank Dr. Masanori Sono for helpful discussions.

REFERENCES

1. Nicolau, K. C., Ritzén, A., and Namoto, K. (2001) Recent developments in the chemistry, biology, and medicine of the epothilones, *Chem. Commun*. 1523−1535.
2. Mühlradt, P. F., Sasse, F. (1997) Epothilone B stabilizes microtubuli of macrophages like taxol without showing taxol-like endotoxin activity, *Cancer Res. 57*, 3344−3346.
3. Rowinsky, E. K., Eisenhauer, E. A., Chaudhry, V., Arbuck, S. G., and Donehower, R. C. (1993) Clinical toxicities excountered with paclitaxel (Taxol), *Semin. Oncol. 21*, 1−15.
4. Kowalski, R. J., Giannakakou, P., and Hamel, E. (1997) Activities of the microtubule-stabilizing agents epothilones A and B with purified tubulin and in cells resistant to paclitaxel (Taxol®), *J. Biol. Chem. 272*, 2534−2541.
5. Chou, T. C., Zhang, X., Harris, C. R., Kuduk, S. D., Balog, A., Savin, K. A., Bertino, J. R., Danishefsky, S. J. (1998) Desoxyepothilone B is curative agasints human tumor xenografts that are refractory to paclitaxel, *Proc. Natl. Acad. Sci. U. S.A. 95*, 15798−15802.
6. Chou, C. T., Zhang, X., Balog, A., Su, D., Meng, D., Savin, K., Bertino, J. R., and Danishefsky, S. J. (1998) Desoxyepothilone B: an efficacious microtubule-targeted antitumor agent with a promising in vivo profile relative to epothilone, *Proc. Natl. Acad. Sci. U.S.A. 95*, 9642−9647.
7. Tang, L., Shah, S., Chung, L., Carney, J., Katz, L., Khosla, C., and Julien, B. (2000) Cloning and heterologous expression of the epothilone gene cluster, *Science 287*, 640−642.
8. Gerth, K., Steinmetz, H., and Reichenbach, H. (2000) Studies on the biosynthesis of epothilones: the biosynthetic origin of the carbon skeleton, *J. Antibiot. 53*, 1373−1377.
9. Nagano, S., Li, H., Shimizu, H., Nishida, C., Ogura, H., Ortiz de Montellano, P. R., and Poulos, T. L. (2003) Crystal structures of epothilone D-bound, epothilone-B bound, and substrate-free forms of cytochrome P450epoK, *J. Biol. Chem. 278*, 44886−44893.
10. Copeland, R. A. (2000) *Enzymes: A Practical Introduction to Structure, Mechanism, and Data Analysis*, 2nd ed., p 311, Wiley-VCH, New York.
11. Pond, A. E., Roach, M. P., Thomas, M. R., Boxer, S. G., and Dawson, J. H. (2001) The H93G Myoglobin cavity mutant as a versatile template for modeling heme proteins: ferrous, ferric, and ferryl mixed-ligand complexes with imidazole in the cavity, *Inorg. Chem. 39*, 6061−6066.
12. Perera, R., Sono, M., Sigman, J. A., Pfister, T. D., Lu, Y., Dawson, J. H. (2003) Neutral thiol as a proximal ligand to ferrous heme iron: implication for heme proteins that lose cysteine thiolate ligation on reduction, *Proc. Natl. Acad. Sci. U.S.A. 100*, 3641−3646.
13. Dawson, J. H., Andersson, L. A., and Sono, M. (1983) The diverse spectroscopic properties of ferrous cytochrome $P450_{cam}$ ligand complexes, *J. Biol. Chem. 258*, 13637−13645.
14. Koo, L. S., Tschirret-Guth, R. A., Straub, W., Moënne-Loccoz, P., Loehr, T. M., and Ortiz de Montellano, P. R. (2000) The active site of the thermophilic CYP119 from *Sulfolobus solfataricus*, *J. Biol. Chem. 275*, 14112−14123.
15. Schalk, M., Batard, Y., Seyer, A., Nedelkina, S., Durst, F., and Werck-Reichhart, D. (1997) Design of fluorescent substrates and potent inhibitors of CYP73As, P450s that catalyze 4-hydroxylation of cinnamic acid in higher plants, *Biochemistry 36*, 15253−15261.
16. Lagueux, J., Affar, E. B., Nadeau, D., Ayotte, P., Dewailly, É., Poirier. G, G. (1997) A microassay for the detection of low levels of cytochrome P450 O-deethylation activities with alkoxyresorufin substrates, *Mol. Cell. Biochem. 175*, 125−129.
17. Chauret, N., Tremblay, N., Lackman, R. L., Gauthier, J. Y., Silva, J. M., Marois, J., Yergey, J. A., and Nicoll-Griffith, D. A. (1999) Description of a 96-well plate assay to measure cytochrome P4503A inhibition in human liver microsomes using a selective fluorescent probe, *Anal. Biochem. 276*, 215−226.
18. Crespi, C. L., and Stresser, D. M. (2000) Fluorometric screening for metabolism-based drug-drug interactions, *J. Pharm. Toxicol. Methods 44*, 325−331.
19. Vernhorst, J., Onderwater, R. C. A., Meerman, J. H. N., Vermeulen, N. P. E., and Commandeur, J. N. M. (2000) Evaluation of a novel high-throughput assay for cytochrome P450 2D6 using 7-methoxy-4-(aminomethyl)coumarin, *Eur. J. Pharm. Sci. 12*, 151−158.
20. Zhang, R., Kang, K. D., Shan, G., and Hammock, B. D. (2003) Design, synthesis and evaluation of novel P450 fluorescent probes bearing α-cyanoether, *Tetrahedron Lett. 44*, 4331−4334.
21. Khan, K. K., and Halpert, J. R. (2002) 7-Benzyloxyquinoline oxidation by P450eryF A245T: finding of a new fluorescent substrate probe, *Chem. Res. Toxicol. 15*, 806−814.
22. Ortiz de Montellano, P. R., and Correia, M. A. (1995) Inhibition of cytochrome P450 enzymes, in *Cytochrome P450: Structure, Mechanism, and Biochemistry* (Ortiz de Montellano, P. R., Ed.) 2nd ed., pp 305−364, Plenum, New York.
23. Estabrook, R. W., Peterson, J., Baron, J., Hildebrandt, A. (1972) in *The Spectrophotometric Measurement of Turbid Suspensions of Cytochromes Associated with Drug Metabolism* (Chignell, C. F., Ed.) Methods in Pharmacology, Vol. 2, pp 303−350, Appleton-Century-Crofts, New York.
24. Davydov, D. R., Hui Bon Hoa, G., and Peterson, J. A. (1999) Dynamics of protein-bound water in the heme domain of P450BM3 studied by high-pressure spectroscopy: comparison with P450cam and P450 2B4, *Biochemistry 38*, 751−761.
25. Hui Bon Hoa, G., Mclean, M. A., and Sligar, S. G. (2002) High pressure, a tool for exploring heme protein active sites, *Biochim. Biophys. Acta 1595*, 297−308.
26. Eliasson, E., Johansson, I., and Ingelman-Sundberg, M. (1990) Substrate-, hormone-, and cAMP-regulated cytochrome P450 degradation, *Proc. Natl. Acad. Sci. U.S.A. 87*, 3225−3229.
27. Cheesman, M. J., Baer, B. R., Zhang, Y. M., Gillam, E. M., and Rettie, A. E. (2003) Rabbit CYP4B1 engineered for high-level expression in *Escherichia coli*: ligand stabilization and processing of the N-terminus and heme prosthetic group, *Arch. Biochem. Biophys. 416*, 17−24.
28. Cupp-Vickery, J., Anderson, R., and Hatziris, Z. (2000) Crystal structures of ligand complexes of P450eryF exhibiting homotropic cooperativity, *Proc. Natl. Acad. Sci. U.S.A. 97*, 3050−3055.
29. Xiang, H., Tschirret-Guth, R. A., and Ortiz de Montellano, P. R. (2000) An Ala245Thr mutation conveys on cytochrome P450eryF the ability to oxidize alternative substrates, *J. Biol. Chem. 275*, 35999−36006.
30. Atkins, W. M., Wang, R. W., and Lu, A. Y. (2001) Allosteric behavior in cytochrome P450-dependent *in vitro* drug-drug interactions: a prospective based on conformational dynamics, *Chem. Res. Toxicol. 14*, 338−347.
31. Hutzler, J. M., Wienkers, L. C., Wahlstrom, J. L., Carlson, T. J., and Tracy, T. S. (2003) Activation of cytochrome P450 2C9-mediated metabolism: mechanistic evidence in support of kinetic observations, *Arch. Biochem. Biophys. 410*, 16−24.
32. Raven, E. L., and Mauk, A. G. (2001) Chemical reactivity of the active site of myoglobin, *Adv. Inorg. Chem. 51*, 1−49.
33. Hiner, A. N., Raven, E. L., Thorneley, R. N., Garcia-Canovas, F., and Rodriguez-Lopez, J. N. (2002) Mechanisms of compound I formation in heme peroxidases, *J. Inorg. Biochem. 91*, 27−34.

BI048980D